JPE 6-3-6

A Novel Sensorless Low Speed Vector Control for Synchronous Reluctance Motors Using a Block Pulse Function-Based Parameter Identification

Ghaderi Ahmad†, Hanamoto Tsuyoshi* and Tsuji Teruo*

†*Graduate School of Life Science and Systems Engineering, Kyushu Institute of Technology, Kitakyushu, Japan

ABSTRACT

Recently, speed sensorless vector control for synchronous reluctance motors (SYRMs) has deserved attention because of its advantages. Although rotor angle calculation using flux estimation is a straightforward approach, the DC offset can cause an increasing pure integrator error in this estimator. In addition, this method is affected by parameter fluctuation. In this paper, to control the motor at the low speed region, a modified programmable cascaded low pass filter (MPCPLF) with sensorless online parameter identification based on a block pulse function is proposed. The use of the MPCLPF is suggested because in programmable cascade low pass filters (PCLPF), which previously have been applied to induction motors, the drift increases vastly when motor speed decreases. Parameter identification is also used because it does not depend on estimation accuracy and can solve parameter fluctuation effects. Thus, sensorless speed control in the low speed region is possible. The experimental system includes a PC-based control with real time Linux and an ALTERA Complex Programmable Logic Device (CPLD), to acquire data from sensors and to send commands to the system. The experimental results show the proposed method performs well, speed and angle estimation are correct. Also, parameter identification and sensorless vector control are achieved at low speed, as well as, as at high speed.

Keywords: dc offset, vector control, synchronous reluctance motors, parameter estimation, MPCLPF, sensorless, low speed

1. Introduction

Synchronous reluctance motors (SYRMs) have several advantages and recently have deserved attention for its use in various industrial applications. To synchronize the stator current vector with rotor position, determination of the rotor position is necessary. While speed sensors increase cost and size, the reliability of the system decreases because of noise effect. Hence recently much research has been done on the sensorless control of SYRM [1-4]. Using armature voltage and current to estimate flux linkage angle is the most straightforward approach and has several advantages, but measurement noise and DC offset causes an increasing error in the pure integrator used in this estimator. Therefore, the estimation of rotor angle and speed is not correct. These incorrect quantities are compared with references variables and cause an unwanted increasing oscillation in flux and torque. Although using a LPF with a large time constant instead of

Manuscript received February 20, 2006; revised May. 22, 2006
†Corresponding Author: ahmad-ghaderi@edu.life.kyutech.ac.jp
Tel: +81-93-695-6053, Fax:+81-93-695-6046, KIT. Kitakyushu
*School of Life Science and Systems Engineering, Kyushu Institute of Technology, Japan.

the pure integrator prevents the output from increasing without bounds, this integrator model becomes inaccurate at low speeds, because the gain and angle of a LPF and a pure integrator will be different, when the frequency reduces to around LPF corner frequency. Thus this method can not solve the above mentioned problem at a low speed region [5-6].

Also estimated rotor position depends on SYRM parameters especially at low speeds, and they must have known accuracy during motor operation [5-7].

To solve aforementioned problems a novel approach for a low speed sensorless vector control of the SYRM which uses a modified programmable cascaded low pass filter (MPCPLF) is proposed [8]. Programmable cascaded low pass filters (PCLPFs) consist of some low pass filter blocks, which reduce drift-error, and an amplifier block in cascade form.

The use of programmable cascaded low pass filters (PCLPFs) instead of pure integrators has previously been applied to the sensorless control of induction motors [9]. However, in this research, an adapted PCLPF was used in the SYRM by using a novel method to avoid of its drawbacks at low speeds. The PCLPF drawbacks have been explained by authors in previous research [10].

Also to avoid parameter variation drawbacks an online parameter identification method which does not depend on estimation accuracy [7, 11] is suggested. In the proposed method, motor parameter identification is done using a block pulse function (BPF) instead of the Euler method which is used in [7, 11]. The BPF increases calculation precision while its computation time is almost the same as the Euler algorithm [12, 13].

Thus sensorless control in the low speed region is achieved using a combination of MPCLPF and BPF-based parameter identification. Since the motor control strategy can be determined by regulating stator current in the d axis, several close loop self control methods, like as constant d-axis current control, maximum torque/ampere control and maximum power factor control are achieved using the identified parameter.

To achieve the proposed method, the experimental setup employs a PC-based system with real time Linux (RTLinux)[14] as an operating system. RTLinux can satisfy the system hardware and software constraints and also real time control can be achieved using this operating system. To acquire the data from the sensors and to send the gate signals to the system, an interface was designed by the Complex Programmable Logic Device (CPLD). The experimental results show the proposed method performs well and speed and angle estimation is correct in a wide range of speeds.

2. Speed sensorless control of SYRM

The block diagram of the proposed sensorless control method is shown in Fig. 1.

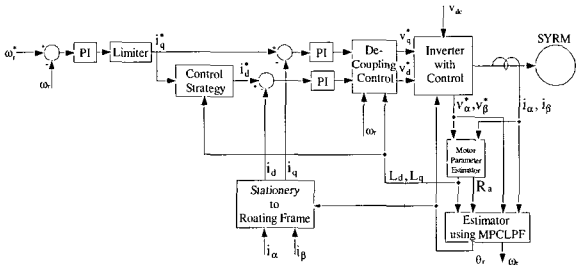

Fig. 1 Block diagram of sensorless speed control of SYRM

Where ρ_s, ω_r, ω_r^*, i_α and i_β are estimated rotor angle, estimated rotor speed, reference rotor speed and armature currents in a stationary reference frame respectively. Also v_d^*, v_q^*, i_d^* and i_q^* are references and i_d, i_q are estimated values in a rotating reference frame respectively. L_d, L_q and R_a are the motor parameters. Here i_q^* is defined by ω_r^* and i_d^* are regulated based on control strategies that are classified by a constant d-axis current, maximum torque per ampere ($i_d^* = i_q^*$) and maximum power factor control ($i_d^* = i_q^* \sqrt{\frac{L_q}{L_d}}$) [16]. The identified stator parameters are used in rotor angle and speed estimation, flux decoupling and i_d^* regulation.

3. Estimation of rotor angle and motor speed

In a SYRM torque (t_e), speed and flux linkage phase angle (ρ_s), in both transient and steady states, can be

calculated by using the estimated stator flux linkage (ψ_s), and its components (ψ_α, ψ_β) in stationary reference frame. The equations of these calculations are shown in (1-5)[5].

$$\psi_\alpha = \int (v_\alpha - R_a i_\alpha)dt \tag{1}$$

$$\psi_\beta = \int (v_\beta - R_a i_\beta)dt \tag{2}$$

$$\rho_s = \tan^{-1}\left(\frac{\psi_\beta}{\psi_\alpha}\right) \tag{3}$$

$$\psi_s = \sqrt{\psi_\alpha^2 + \psi_\beta^2} \tag{4}$$

$$t_e = \frac{3}{2} p(\psi_\alpha i_\beta - \psi_\beta i_\alpha) \tag{5}$$

Where p is number of poles.

As seen in the above equations when equations (1) and (2) are used for flux calculation, noise or DC offset in measured currents, make an increasing error in flux estimation.

Using a PCLPF instead of a pure integrator is an approach that has been previously proposed to solve same problems in sensorless control of induction motors [9]. Because a PCLPF includes some LPF blocks and each LPF decreases the effect of the DC-offset, the DC-offset effect in the PCLPF output decreases effectively. In a PCLPF, the cutoff frequency of the low pass filters and amplifier gain are a function of the stator frequency. Therefore, in each frequency, the PCLPF acts as a pure integrator, meanwhile, DC offset problems can be solved.

The transfer function of a three stage low pass filer which defined by H(s) is represented in (6)-(8).

$$\tau = \frac{1}{\omega_e} tan\left(\frac{\pi}{6}\right) \tag{6}$$

$$G = \frac{1}{\omega_e}\sqrt{\left[1+(\omega_e\tau)^2\right]^3} = \frac{8}{3\sqrt{3}}\frac{1}{\omega_e} \tag{7}$$

$$H(s) = G\left(\frac{1}{\tau s+1}\right)^3 \tag{8}$$

Where ω_e, G and τ are the supplied voltage frequency, the PCLPF gain and the time constant of cascaded filters respectively.

As a result, the estimated fluxes of both axes ($\hat{\psi}_\beta$, $\hat{\psi}_\alpha$) and phase angle ($\hat{\rho}_s$) are calculated as follows using (8) instead of (1)-(3).

$$\hat{\psi}_\alpha = (v_\alpha - R_a i_\alpha)H(s) \tag{9}$$

$$\hat{\psi}_\beta = (v_\beta - R_a i_\beta)H(s) \tag{10}$$

$$\hat{\rho}_s = \tan^{-1}\left(\frac{\hat{\psi}_\beta}{\hat{\psi}_\alpha}\right) \tag{11}$$

However, the PCLPF may make some problems at low speeds because the drift is proportional to the PCLPF gain and it increases vastly. As a result, the estimated value will be invalid and sensorless control will not be achieved at low speeds [10].

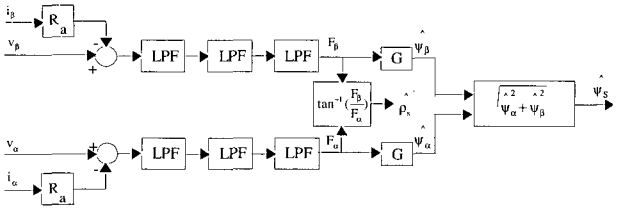

Fig. 2 Proposed estimation method

To avoid these disadvantages, we propose a modified PCLPF (MPCLPF) shown in Fig.2. In this new method the output is extracted just after three stages of the LPF, in calculation of stator flux linkage phase angle ($\hat{\rho}_s'$). Because gain (G shown in Fig 2) is a common factor in ψ_α and ψ_β, it can be eliminated in phase angle calculation. Hence $H'(s)$, which is defined as MPCLPF transfer function and shown in (12), is used instead of (8).

$$H'(s) = \left(\frac{1}{\tau s+1}\right)^3 \tag{12}$$

And in equation (15), in order to calculate $\hat{\rho}_s'$ the output of the MPCLPF, Which is shown in (13) and (14), is used instead of (9) and (10).

$$F_\alpha = (v_\alpha - R_a i_\alpha)H'(s) \tag{13}$$

$$F_\beta = (v_\beta - R_a i_\beta)H'(s) \tag{14}$$

$$\hat{\rho}_s = \tan^{-1}\left(\frac{F_\beta}{F_\alpha}\right) \quad (15)$$

Where F_α and F_β are defined as the output of the third LPF in the α and β axes, respectively.

To calculate rotor angle (θ_r), the vector diagram of the motor fluxes, as shown in Fig.3, is used. The relationship between θ_r, load angle (δ) and ρ_s, which is presented in

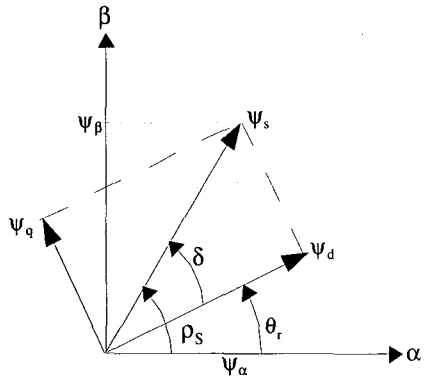

Fig. 3 Flux vector diagram

(16), are extracted using this figure.

$$\theta_r = \rho_s - \delta \quad (16)$$

And also from Fig.3 (17)-(18) can be written.

$$\psi_d = |\psi_S|\cos\delta = L_d i_d \quad (17)$$

$$\psi_q = |\psi_S|\sin\delta = L_q i_q \quad (18)$$

Finally load angle can be extracted in (20) by considering (17)-(19) and Fig.3.

$$i_s = \sqrt{i_\alpha^2 + i_\beta^2} \quad (19)$$

$$\delta = sin^{-1}\left[\left[\frac{L_q^2|i_s|^2/|\psi_s|^2 - L_q^2/L_d^2}{1 - L_q^2/L_d^2}\right]^{\frac{1}{2}}\right] \quad (20)$$

Because δ is assumed almost invariable at constant loads and its variation rate is considered small compared to ρ_s. Motor speed (ω_r) is calculated using ρ_s as follows:

$$\omega_r = \frac{d}{dt}\theta_r \approx \frac{d}{dt}\rho_s \quad (21)$$

In the proposed method, rotor angle estimation is not directly dependent on the motor speed. Therefore, at low speeds the estimated and actual rotor positions are in agreement. It is possible to control the motor in a wide range of speeds and vector control is achieved at low speeds, as well as high speeds.

4. On line parameter identification using block pulse function

4.1 Variation of armature resistance at low speed

In rotor angle calculation using estimated stator flux linkage, as seen in equations (13)-(20), the rotor angle estimation is dependent on armature inductance and armature resistance. Thus, any variation in motor parameters will disorder position estimation. The effect of stator resistance variation is more important in low speed regions, because the inverter voltage decreases in relation to stator resistance voltage and the resistance voltage dominates the integrator input in low speed [5, 8].

On the other hand to avoid using voltage transducers, the actual voltage is not measured and the reference voltage is used in the phase angle estimation. However, the nonlinearity of the PWM inverter, caused by dead-time effect, on-state voltage drop and threshold voltage of the power semiconductor switches, make the machine terminal voltages different from reference voltages when motor speed and the amplitudes of the stator voltages are low [6].

Since the main aim is phase angle estimation, armature resistance and nonlinearity of the inverter having the same effect on rotor angle estimation, the effect of these nonlinearities can be compensated, by assuming it as an additional nonlinear resistance series with armature. Therefore the identified resistance includes armature resistance and the effect of power switch nonlinearity. Therefore for proper rotor angle estimation this resistance should be identified during motor operation.

4.2 Parameter identification using block pulse function

To identify the parameters in sensorless control, the circuit equation of the SYRM in actual d-q, which is represented in equation (22), will be transformed to an

estimated rotating coordinate, which is defined here as $\delta-\gamma$, using (23) and (24).

$$\begin{bmatrix} v_d \\ v_q \end{bmatrix} = \begin{bmatrix} R_a + PL_d & -\omega_r L_q \\ \omega_r L_d & R_a + PL_q \end{bmatrix} \begin{bmatrix} i_d \\ i_q \end{bmatrix} \tag{22}$$

$$\begin{bmatrix} v_\gamma \\ v_\delta \end{bmatrix} = \begin{bmatrix} \cos\Delta\theta & -\sin\Delta\theta \\ \sin\Delta\theta & \cos\Delta\theta \end{bmatrix} \begin{bmatrix} v_d \\ v_q \end{bmatrix} \tag{23}$$

$$\begin{bmatrix} i_\gamma \\ i_\delta \end{bmatrix} = \begin{bmatrix} \cos\Delta\theta & -\sin\Delta\theta \\ \sin\Delta\theta & \cos\Delta\theta \end{bmatrix} \begin{bmatrix} i_d \\ i_q \end{bmatrix} \tag{24}$$

Where $\Delta\theta$ is the angle difference of actual d-q axes and the estimated $\delta-\gamma$ axes.

Finally, the space state form of the SYRM which includes motor parameter matrices is extracted in (25). And the equations of parameter matrices, which are defined as A and B, and motor parameters are shown in (26)-(31).

$$\frac{d}{dt}\begin{bmatrix} i_\gamma \\ i_\delta \end{bmatrix} = A\begin{bmatrix} i_\gamma \\ i_\delta \end{bmatrix} + B\begin{bmatrix} v_\gamma \\ v_\delta \end{bmatrix} \tag{25}$$

$$\begin{aligned} A = \begin{bmatrix} a_{11} & a_{12} \\ a_{21} & a_{22} \end{bmatrix} &= \frac{-R_a(L_d+L_q)}{2L_dL_q}\begin{bmatrix} 1 & 0 \\ 0 & 1 \end{bmatrix} + \\ &\frac{R_a(L_d-L_q)}{2L_dL_q}\begin{bmatrix} \cos 2\Delta\theta & \sin 2\Delta\theta \\ \sin 2\Delta\theta & -\cos 2\Delta\theta \end{bmatrix} \\ &+\frac{\omega_{re}}{L_dL_q}\begin{bmatrix} M_{11} & M_{12} \\ M_{21} & M_{22} \end{bmatrix} \end{aligned} \tag{26}$$

$$\begin{aligned} B = \begin{bmatrix} b_{11} & b_{12} \\ b_{21} & b_{22} \end{bmatrix} &= \frac{(L_d+L_q)}{2L_dL_q}\begin{bmatrix} 1 & 0 \\ 0 & 1 \end{bmatrix} \\ &-\frac{(L_d-L_q)}{2L_dL_q}\begin{bmatrix} \cos 2\Delta\theta & \sin 2\Delta\theta \\ \sin 2\Delta\theta & -\cos 2\Delta\theta \end{bmatrix} \end{aligned} \tag{27}$$

$$M_{11} = \frac{1}{2}\sin 2\Delta\theta\,(L_d^2 - L_q^2) \tag{28}$$

$$M_{12} = \frac{1}{2}\left[(L_d^2 + L_q^2) + \cos 2\Delta\theta\,(L_d^2 - L_q^2)\right] \tag{29}$$

$$M_{21} = -\frac{1}{2}\left[(L_d^2 + L_q^2) + \cos 2\Delta\theta\,(L_d^2 - L_q^2)\right] \tag{30}$$

$$M_{22} = -\frac{1}{2}\sin 2\Delta\theta\,(L_d^2 - L_q^2) \tag{31}$$

Where ω_{re} is angular velocity at electrical angle.

In this paper, to satisfy estimation validity, the authors suggest an online motor parameter identification using block pulse function (BPF) which is achieved by extracting A and B from the equation (25).

BPF is a set of orthogonal functions with piecewise constant values that are shown in equation (32) and (33) [12].

$$\phi_i(t) = \begin{cases} 1 & for\ (i-1)\dfrac{T}{m} \le t \le \dfrac{iT}{m} \\ 0 & otherwise \end{cases} \tag{32}$$

$$\Phi(t) = [\phi_1(t)\ \phi_2(t)\ \ldots\ldots\phi_i(t)\ \ldots\ldots\phi_m(t)] \tag{33}$$

Where m is an arbitrary positive integer and T is the final time. Also h is defined as $h = \dfrac{T}{m}$.

To use the BPF approximation, differential equations are transformed approximately into their corresponding algebraic forms based on the operation rules of the BPF, so that the numerical solutions are obtained more directly. The proposed method increases calculation precision compared with the Euler method [12, 13].

To estimate the unknown parameter matrices using the BPF, its space states should be expanded into a block pulse series.

$$\dot{X}(t) = AX(t) + BU(t) \tag{34}$$

$$X(t) \approx [x_1\ x_2\ \ldots\ldots x_k\ \ldots\ldots x_m]\Phi(t) = X\Phi(t) \tag{35}$$

$$U(t) \approx [u_1\ u_2\ \ldots\ldots u_k\ \ldots\ldots u_m]\Phi(t) = U\Phi(t) \tag{36}$$

Where $X(t)$, $U(t)$, x_k and u_k are a matrix of input , a matrix of output and their average values over the sampling period respectively.

All the (m-1) equations in (34) can be expressed in a matrix form as follows.

$$\theta^T = (A\ B) \tag{37}$$

$$G^T = \frac{h}{2}\begin{pmatrix} x_{k+1} + x_k \\ u_{k+1} + u_k \end{pmatrix} \tag{38}$$

$$F^T = [x_{k+1} - x_k] \tag{39}$$

$$F = G\theta \tag{40}$$

And finally the system parameter matrixes are identified using (41).

$$\theta = (G^T G)^{-1} G^T F \tag{41}$$

To identify the motor parameter matrix, phase currents are defined as input matrix, while the voltages are an output matrix in equations (42) and (43). Since the direct computations of (40) need a large memory size it should be solved recursively, as shown in (44)-(45).

$$X = \left[i_\gamma \; i_\delta\right]^T \tag{42}$$

$$U = \left[v_\gamma \; v_\delta\right]^T \tag{43}$$

$$X_{k+1} = \Gamma\left(\left(I + \frac{h}{2}A\right)X_k + \frac{h}{2}B\left(U_{k+1} + U_k\right)\right) \tag{44}$$

$$\Gamma = \left(I - \frac{h}{2}A\right)^{-1} \tag{45}$$

Where I is the unit matrix.

Thus (25) is transformed approximately into its BPF corresponding algebraic forms, which are shown in (46).

$$\begin{bmatrix} i_{\gamma(k+1)} - i_{\gamma(k)} \\ i_{\delta(k+1)} - i_{\delta(k)} \end{bmatrix} = \frac{h}{2}A\begin{bmatrix} i_{\gamma(k+1)} + i_{\gamma(k)} \\ i_{\delta(k+1)} + i_{\delta(k)} \end{bmatrix} + \frac{h}{2}B\begin{bmatrix} v_{\gamma(k+1)} + v_{\gamma(k)} \\ v_{\delta(k+1)} + v_{\delta(k)} \end{bmatrix} \tag{46}$$

Equation (46) is a derived relation between the voltages and currents in a block pulse regression equation. This is used to identify unknown parameter matrices using a recursive least square algorithm which efficiently reduces computation size. To calculate motor parameter, the following equations are used [7, 11].

$$M_1 = a_{11} + a_{22} = \frac{L_d + L_d}{L_d L_q} \tag{47}$$

$$M_2 = b_{11} + b_{22} = \frac{-R_a(L_d + L_d)}{L_d L_q} \tag{48}$$

$$M_3 = \sqrt{(b_{11} - b_{22})^2 + 4b_{12}b_{21}} = \frac{-(L_d - L_d)}{L_d L_q} \tag{49}$$

$$R_a = -\frac{M_2}{M_1} \tag{50}$$

$$L_d = \frac{2}{M_1 - M_3} \tag{51}$$

$$L_q = \frac{2}{M_1 + M_3} \tag{52}$$

As shown in equations (47)-(52) although parameter matrixes (A,B) include $\Delta\theta$, the identified parameter is not dependent on $\Delta\theta$. Hence, in this method, parameter identification is not affected by position estimation accuracy [11].

5. Experimental setup

To realize the validity of the control theory a PC-based control system is used in the experimental setup. Since, there is need for an appropriate operating system with real time control ability, the Real Time Linux (RTLinux) is used in this system. The RTLinux is a hard real-time operating system that handles time-critical tasks and runs the normal Linux as its lowest priority execution thread [14].

The experimental setup, which employs RTiC-Lab, includes a graphic user interface, remote monitoring and networking [17]. Therefore it is possible to monitor motor variables and change its reference variables or its control method strategy instantaneously during motor operation. This system consists of a Complex Programmable Logic Device (CPLD), 10MHz system clock and A/D converter. An ALTERA FLEX10K50 [18] is selected for CPLD device and the circuit is designed using VHDL. The speed and position detectors with speed correction function, clock the generator for the A/D converter and the ISA interface circuit are designed in it.

Fig.4 and Fig.5 show the RTLinux-based experimental system. As seen in Fig.4 currents are sampled by analog to digital converter and link to the PC via the CPLD. The PWM inverter is driven by gate signals which are made by the PWM signal generator. The PC system is connected to the CPLD using the ISA Bus. The nominal parameter of the SYRM is shown in the Table 1.

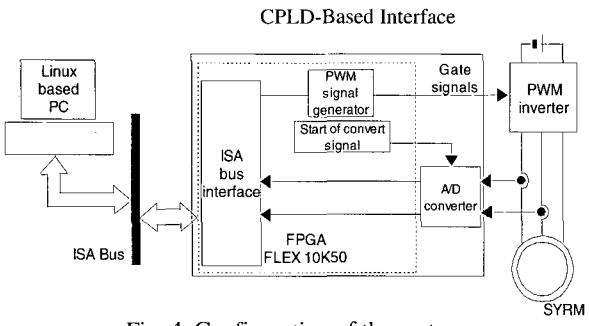

Fig. 4 Configuration of the system

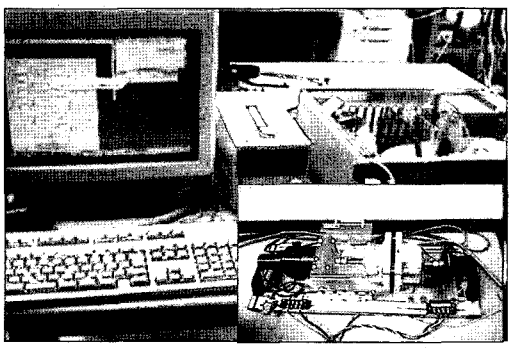

Fig. 5 Experimental Setup

Table 1 SYRM Motor Nominal Parameters

Rated Power	86W
Rated Torque	0.4 Nm
Rated Current	1.7A rms
d Axis Armature inductance at rated current	93 mH
q Axis Armature Inductance at rated current	36 mH
Inverter Voltage	150 V
Pole	4
Armature Resistance (R_a)	1.89 Ω

6. Experimental results

The experimental results which are obtained at 100 rpm, 600 rpm and 1200 rpm are shown in Fig. 6-11. These results show, sensorless vector control is achieved at low speed regions, as well as, at high speeds using the proposed method. Fig. 6 and Fig. 7 show the identified parameter. As seen in this figures, the effect of the inverter nonlinearity increases at low speeds and this effect is considered an additional nonlinear resistance series with armature circuit. The identified resistance in 100 rpm is grater than in cases of 600 rpm.

Also, as seen in Fig. 8 and Fig. 9, the estimated rotor angle agrees with the actual rotor angle and the accuracy of the angle estimation, which is shown by $\Delta\theta$, is acceptable at high and low speeds.

To test the estimation robustness again the DC offset, 25 mA was added to the motor current signals while the motor was operating at 20 percent of rated torque, and as shown in Fig.10 even in these conditions, rotor angle estimation and sensorless control is achieved.

Although estimation using the MPCLPF is based on study state equations, the experimental result of the transient response in Fig. 11 shows sensorless control can be achieved when a step change is applied to the reference speed. In which case, rotor angle estimation and system transient response are acceptable.

The experimental results of the maximum power factor and maximum torque per ampere controls which are shown in Fig.12 and Fig.13 prove these control strategies can be achieved using the proposed method. As seen in these figures, the d axis current is set based on a control strategy and the d-q axes currents in the estimated and actual reference frame is in agreement.

7. Conclusions

In this paper, a novel sensorless speed control for a SYRM is proposed. In this method to solve drift problems and motor parameter fluctuation in phase angle estimation, a MPCLPF with an online identification method based on block pulse function is proposed. The experimental results show the rotor angle and speed estimations and parameter identification performs well. Sensorless control with a self control strategy is achieved at low speeds as well as, at high speeds.

References

[1] T. Tamamura, Y. Honda, S. Morimoto, Y .Takeda, "Synchronous Reluctance motor when used Air-Condition Compressor Motor, a comparative study," Proc. of the IPEC-Tokyo 2000, pp. 654-659.

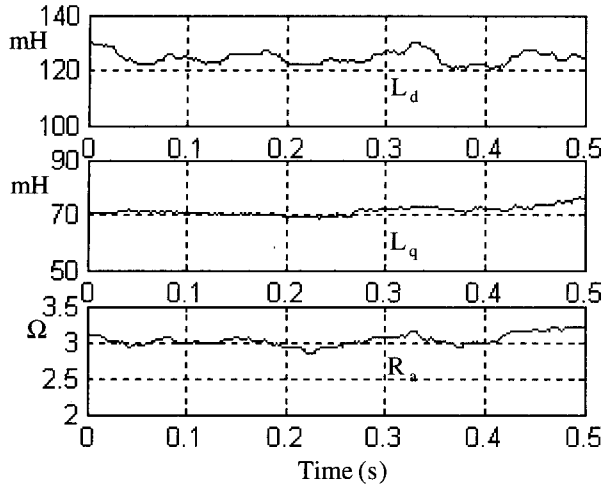

Fig. 6 Identified motor parameters at 100 rpm

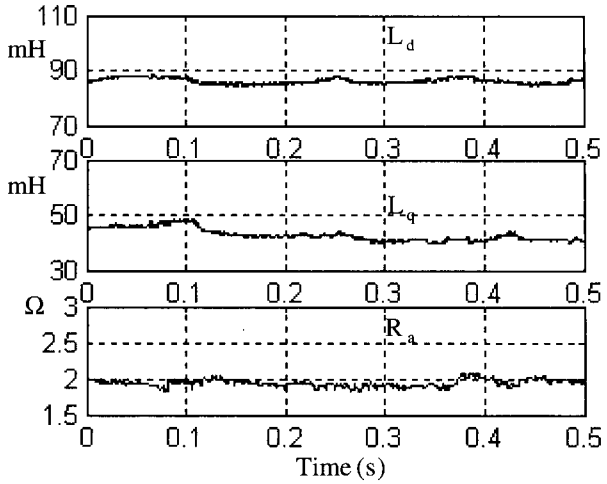

Fig. 7 Identified motor parameters at 600 rpm

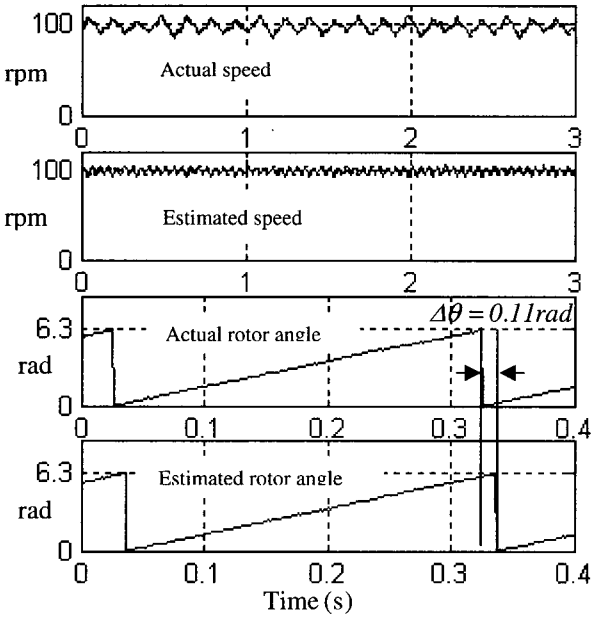

Fig. 8 Experimental results at 100 rpm

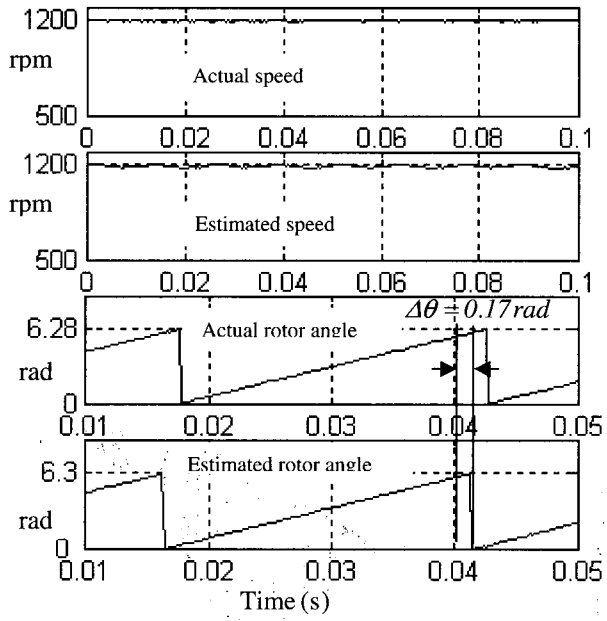

Fig. 9 Experimental results at 1200 rpm

[2] T. Hanamoto, A. Ghaderi, T. Fukuzawa, T. Tsuji, "Sensorless control of synchronous reluctance motor using modified flux linkage observer with an estimation error correct function," Proc. of the ICEM-2004,Sep 2004, Include CD-ROM.

[3] C-G. Chen, T-H. Liu, M-T. Lin, C-A. Tai, "Position control of a sensorless synchronous reluctance motor" IEEE Transactions on Industrial Electronics, 2004, vol. 51, No. 1, pp. 15-25.

[4] S. Saha, T. Iijima, K. Narazaki, Y. Honda, "High speed sensorless control of synchronous reluctance motor by modulating the flux linkage angle," Proc of IPEC-Tokyo 2000, 2000, pp.643-648.

[5] P. Vas, Sensorless vector and direct torque control, Oxford University Press, 1998.

[6] J. Holtz, "Developments in sensorless AC drive technology" proc of IEEE PEDS-Kuala Lumpur 2005, 2005, pp 9-16.

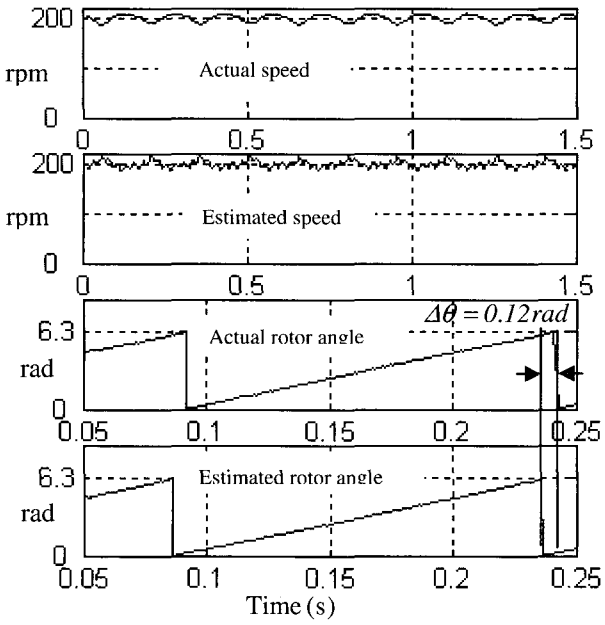

Fig. 10 Experimental results whit 25 mA artificial dc offset

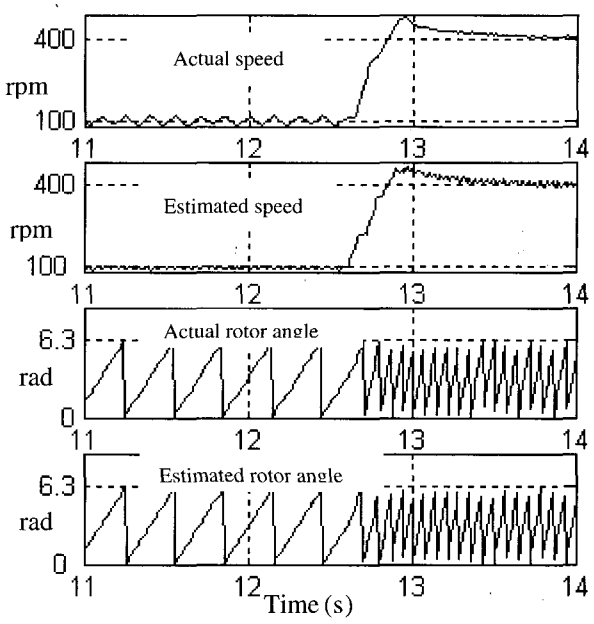

Fig. 11 Experimental results of transient response

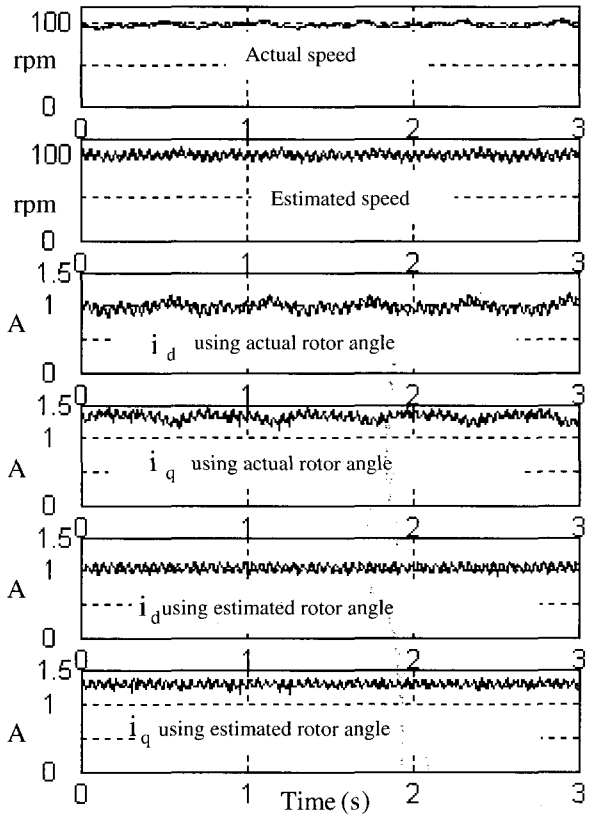

Fig. 12 Experimental results of maximum power factor control

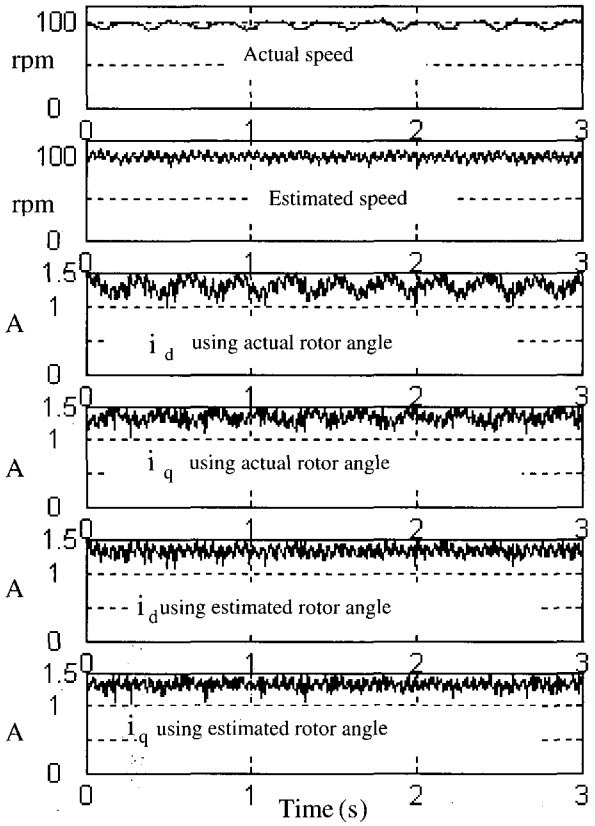

Fig. 13 Experimental results of maximum torque per ampere control

[7] S. Ichikawa, A. Iwata, M. Tomita, S. Doki, S. Okuwa, "Sensorless control of synchronous reluctance motors using an on-line parameter identification method taking into account magnetic saturation" proc of the PESC 04,2004, pp. 3311-3316.

[8] A. Ghaderi, T. Hanamoto, T. Tsuji, "A novel implementation method of a programmable cascaded Low pass filters for a low speed sensorless control of synchronous reluctance motors" proc of IEEE PEDS-Kuala Lumpur 2005, 2005, pp 360-365.

[9] B.K. Bose, N.R. Patel, "A programmable cascaded low-pass filter based Flux synthesis for a stator flux-oriented vector-controlled Induction motor drive," IEEE Transaction on Industrial Electronics, Vol. 44., No. 1, pp.140-143, February 1997.

[10] A. Ghaderi, M. Ebrahimi, T. Hanamoto, "A novel compensation method of the flux estimation error in a stator flux oriented vector control of induction motors", Proc of ICEE-Sapporo, 2004, pp.193-198.

[11] A. Iwata, S. Ichikawa, M. Tomita, S. Doki, S. Okuwa, "Sensorless control of synchronous reluctance motors using an on-line parameter identification not affected by position estimation accuracy" IEEJ Transaction on Industry Application" Vol.124, No.12, pp.1205-1211, 2004. (Japanese)

[12] Zhihua Jiang, Walter Schaufelberger "Block Pulse Functions and Their Applications in Control Systems" Springer-Verlag, 1992.

[13] T. Hanamoto, A. Ghaderi, T. Tsuji, "RTLinux Based Online Real Time Simulator of SPMSM using the Block Pulse Approximation" proc of IEEE PEDS-Kuala Lumpur 2005, 2005, pp 1118-1122.

[14] http://www.rtlinux.org

[15] T. Hanamoto, A. Ghaderi, T. Tsuji ,"Sensorless speed control of cylindrical type PMSM using modified flux observer" Proc. of IPEC-Niigata 2005,2005, pp. 1011–1015.

[16] B. K. Bose, "Modern power electronics and drives", Prentice Hall PTR, 2002.

[17] http://rtic-lab.sourceforge.net/

[18] http://www.altera.com

Ahmad ghaderi received his B.S. and M.S. in Electrical Engineering from Shahed University and Isfahan University of technology, Iran, in 1999 and 2002 respectively. From 2002 to 2003 he was with National Iranian Oil Refining and Distribution Company. He has been a Ph.D. Student in Electrical Engineering in Kyushu Institute of Technology, Japan, since 2003. His research interests include motor control and power electronics.

Tsuyoshi Hanamoto received his B.S. and M.S. from Kyushu Institute of Technology, Japan, in 1984 and 1986, respectively. In 1986 he joined Kobe works of Kobe Steel, Ltd. In 1990 he was engaged Center for Cooperative Research of Kyushu Institute of Technology. From 1997 to 2000 he was with the Department of Electrical Engineering. Since April 2000 he has been with the Graduate School of Life Science and Systems Engineering, Kyushu Institute of Technology, where he is presently an Associate Professor. His research interests include motor control and power electronics.

Teruo Tsuji received his B.S., M.S., and Dr. Eng. Degrees in Electrical Engineering from Kyushu University, Japan, in 1963, 1965 and 1978 respectively. From 1968 to 2001 he was with the Department of Electrical Engineering, Kyushu Institute of Technology. Since 2001 he has been with the Graduate School of Life Science and Systems Engineering, Kyushu Institute of Technology, where he is presently a Professor. His research interests include control, identification, and control application to magnetic levitation system and power electronics systems.